Mandelbrot Geometry and Stability in Population Growth Models

Extended Essay in Mathematics Analysis and Approaches HL

Research Question:

How do the period-n bulbs of the Mandelbrot set correspond to stability regions in the bifurcation diagram of the logistic map?

Student number:
Word Count: 3,998

Contents

1 Introduction

The study of non-linear dynamical systems is key to understand and analyse real-world phenomena through the lens of abstract mathematics. Creating a concrete link between applied areas of mathematics as well as very analytical ones. An example of such connections is the relationship of population dynamics (represented by the logistic map) with the Mandelbrot set.

The Mandelbrot set contains infinitely many n-periodic regions, where the behaviour of the system repeats itself in cycles of length n. In a similar way, the bifurcation diagram of the logistic map demonstrates stability windows of a dynamic system, which are intervals where the system settles into a repeating pattern. The strong visual similarity between these two structures suggests that a deeper mathematical correspondence exists between them.

This essay investigates this connection by addressing the Research Question:

> **How do the period-n bulbs of the Mandelbrot set correspond to stability regions in the bifurcation diagram of the logistic map?**

By combining analytical conjugacy between the two dynamical systems with computational and numerical work and verification of stability windows, this work aims to demonstrate that the logistic map and the Mandelbrot set are linked through a direct parameter transformation. Establishing this link highlights how abstract and complex fractal geometry can connect to real models of population dynamics.

2 Background

2.1 Mandelbrot set

2.1.1 Fractals

Fractals are mathematical objects characterised by their self-similarity on different scales. They are generally generated through iterative applications of simple processes, such as a recursive function, resulting in structures with complex and infinite details. The complexity of such structures results in their boundaries being often difficult to describe rigorously, leading them to possess non-integer dimensions [1]. Their connection to dynamic systems makes them a central subject in the study of chaos. [2]

2.1.2 Definition and examples

The Mandelbrot set, first defined in 1979 by Robert W. Brooks and Peter Matelski [2], is a fractal defined as the set of all complex numbers c for which the iteration

$$z_{n+1} = z_n^2 + c, \quad z_0 = 0, \quad \text{(also denoted } P_c(z_n)\text{)} \tag{1}$$

remains bounded as $n \to \infty$. [3]. Boundedness in this context is defined as the modulus of z_n (noted $|z_n|$) staying finite. We define the orbit of a number under an iterative application as the sequence of values

$$z_0, z_1, z_2, z_3, \ldots, z_n,$$

written

$$O(c) = \{z_n\}_{n=0}^{\infty}.$$

We can therefore talk about boundedness as the orbit staying bounded in value. [4]

Looking at the example where $c = -1$, we can apply the Mandelbrot function to it and find:

$$\begin{aligned} z_0 &= 0, \\ z_1 &= 0^2 - 1 = -1, \\ z_2 &= (-1)^2 - 1 = 0, \\ &\ldots \end{aligned} \tag{2}$$

It can be shown that, if the orbit of $z_0 = 0$ under $f(z_{n+1}) = z_n^2 + c$ is periodic (repeats itself), then it is bounded and, therefore, c is in the Mandelbrot set (noted $\mathbb{M}$) [5]. In the case where $c = -1$ (2), because the repetition appeared after 2 steps, we say that the orbit of c has a period of 2 and that c is part of the period-corresponding bulb of $\mathbb{M}$ [6].

Note that (1) can be applied to complex values of c. This is relevant as the fractal under analysis here takes form on the complex plane, making the analysis of complex numbers under this application particularly appropriate.

Looking at $c = i + 1$ gives,

$$\begin{aligned} z_0 &= 0 & |z_0| &= 0, \\ z_1 &= 1 + i & |z_1| &= \sqrt{2}, \\ z_2 &= 1 + 3i & |z_2| &= \sqrt{10}, \\ z_3 &= -7 + 7i & |z_3| &= \sqrt{98}, \\ z_4 &= 1 - 97i, & |z_4| &= \sqrt{94010}, \\ &\ldots & &\ldots \end{aligned} \tag{3}$$

Observe that the modulus of z_n does not stay bounded and grows indefinitely, implying that $c = i + 1$ is not part of $\mathbb{M}$.

2.1.3 Visualisation

In order to visualise the Mandelbrot set, the points of the complex plane inside $\mathbb{M}$ have to be visibly distinguished from the rest (see Fig.1).

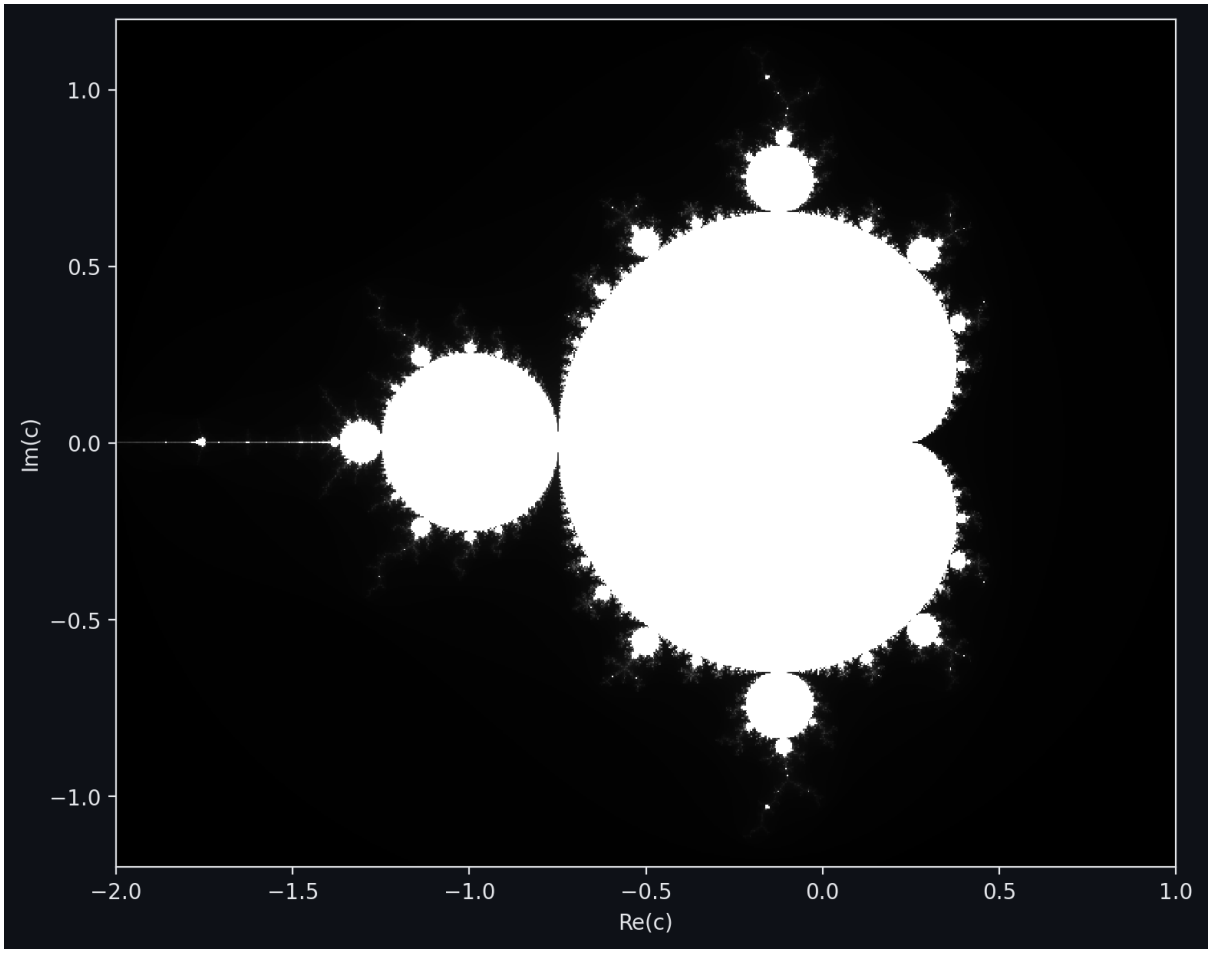

Figure 1: Visualisation of the Mandelbrot set, showing points coloured according to membership in $\mathbb{M}$. (From: author's own visualisation, generated in Python [7])

2.1.4 Hyperbolic components and period-n bulbs

When investigating the structure of the Mandelbrot set, one could look at the orbit of a point c (as done above), but looking at the periodicity of that orbit reveals further important patterns. Regions with the same periodicity are called *hyperbolic components* and form well-defined "bulbs" attached to the main cardioid of the set (see Fig.2).

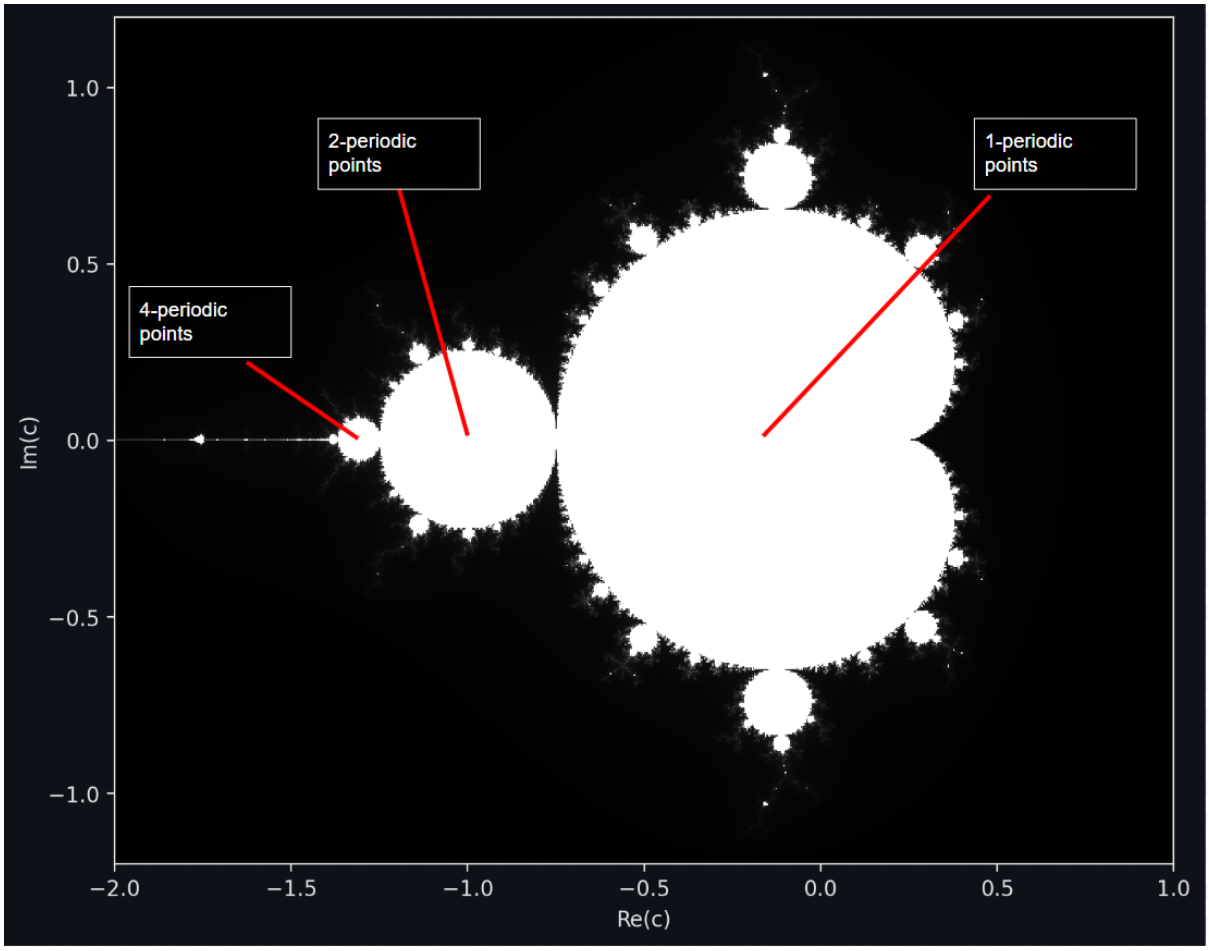

Figure 2: Periodicity of points in the bulbs of the Mandelbrot set, labelled by their cycle's periodicity. From: Author's own visualisation [7]

Definition: A *hyperbolic component* is a connected region of parameter space for which the repetitive iteration $P_c(z) = z^2 + c$ admits a periodic cycle (called attracting cycle) such as the one in (2) [8] [9] [10]. The reason for their use in this investigation is that these regions are precisely the visible bulbs in Mandelbrot visualisations [6], and they describe where the dynamics are structurally stable [11].

The limitation of such components in the context of the Mandelbrot set is that, on the boundary of a hyperbolic component, the cycle is no longer attracting, which introduces more delicate behaviour which will not be explored in this essay [12].

Each hyperbolic component is labelled by the period of its attracting cycle (see Fig.2). The result is the family of period-n bulbs, where each bulb corresponds to parameters c for which the orbit of the critical point ($O(c)$) converges to an attracting cycle of period n [13]. This classification will help visualise how such periodicity in the Mandelbrot set relates to the logistic map.

The notion of periodic hyperbolic components allows us to rigorously compare the structure of the Mandelbrot set with the logistic map (2.2). This terminology will be used extensively when addressing the research question of this investigation (4.1).

2.2 Logistic map

2.2.1 Definition and Origin

The logistic map is a discrete-time recurrence relation that models the evolution of a population under constrained growth. It is defined as:

$$x_{n+1} = rx_n(1 - x_n) \quad \text{(also denoted } f_r(x_n)\text{)}, \tag{4}$$

where $x_n \in [0, 1]$ represents the normalised population at time step n relative to the maximum sustainable population (called carrying capacity) and $r > 0$ is the growth parameter [14]. In this model, the term x_n accounts for the proportional growth of the population, while $(1-x_n)$ introduces a limiting factor (which could represent real-life limitations like finite resources), hence reducing the growth as x_n approaches the carrying capacity. [15]

The logistic map arises from the logistic growth differential equation,

$$\frac{dP}{dt} = rP(1 - \frac{P}{K}), \tag{5}$$

where P is the population at continuous time t, and K is the carrying capacity, which was first proposed in 1838 by the Belgian mathematician Pierre François Verhulst to describe population growth limited by environmental constraints [16]. In the logistic map (4), this (5) equation is discretised, giving the logistic map a simpler non-linear iterative model. [17]

While its development was originally aimed towards population modelling, the logistic map was linked to chaos theory in the 1970s, leading to it being studied extensively by mathematicians such as Robert May and Mitchell Feigenbaum [18]. Robert May's 1976 paper demonstrated that varying the parameter r leads to a range of dynamical behaviour; the stability of the system shifting drastically from periodic oscillations to chaos [19]. The sensitivity of the logistic map relates directly to the stability analysis of population growth models. The relationship between the logistic map and stability analysis becomes particularly relevant when attempting to link it to the Mandelbrot set (4.1).

In the context of iterative maps such as (4), we define the period k of a cycle refers to the number of iterations required for the system to return to a previous state. A point x^* has period k if $f_r^{(k)}(x^*) = x^*$ and k is the smallest positive integer with this property, where $f_r^{(k)}$ denotes the value of $f_r(x)$ after k steps [20]. The case $k = 1$ corresponds to fixed points, where the value of the system remains constant over time (see 2.2.2).

2.2.2 Fixed points and stability

For the logistic map (4), a fixed point is a value x^* such that $x_{n+1} = x_n = x^*$. Setting $x_{n+1} = x_n$ in the recurrence gives:

$$x^* = rx^*(1 - x^*) = rx^* - r(x^*)^2$$

$$\therefore 0 = rx^* - r(x^*)^2 - x^*$$

$$\therefore 0 = x^*(r - rx^* - 1) = x^*(r(1 - x^*) - 1)$$

giving two fixed points:

$$x_0^* = 0, \quad x_1^* = 1 - \frac{1}{r}.$$

The *stability* of a fixed point is determined by the derivative of the iteration function

$$f_r(x) = rx(1 - x), \tag{6}$$

evaluated at x^*. A fixed point is stable if

$$|f_r'(x^*)| < 1. \tag{7}$$

This condition (7) follows from linearising the map near x^*: if a small perturbation ϵ_n is applied to the system, the next iteration changes it by approximately $\epsilon_{n+1} \approx f_r'(x^*)\,\epsilon_n$. When $|f_r'(x^*)| < 1$, the perturbation decreases in magnitude over multiple iterations, therefore, causing trajectories to return to x^*, in turn, ensuring stability. On the other hand, if $|f_r'(x^*)| > 1$, the perturbations grow over iterations, and the fixed point is unstable. [21]

Since

$$f_r'(x) = r(1 - 2x),$$

we have:

- For $x_0^* = 0$: $f_r'(0) = r$. The stability condition $|r| < 1$ implies that the origin is stable for $0 < r < 1$.
- $x_1^* = 1 - \frac{1}{r}$:

$$f_r'\left(1 - \frac{1}{r}\right) = r\left(1 - 2\left(1 - \frac{1}{r}\right)\right) = -r + 2.$$

The stability condition $|-r + 2| < 1$ gives $1 < r < 3$.

Thus:

- For $0 < r < 1$, the population tends to extinction ($x = 0$ being the stable point it converges to).
- For $1 < r < 3$, the population approaches a non-zero equilibrium expressed by $x = 1 - \frac{1}{r}$.
- At $r = 3$, the fixed point x_1^* loses stability, leading to a *period-doubling bifurcation* (see Section 2.2.3).

These results mark the first stability window in the bifurcation diagram of the logistic map, corresponding to a period-1 region. This can be confirmed when plotting the bifurcation diagram (see Fig.3):

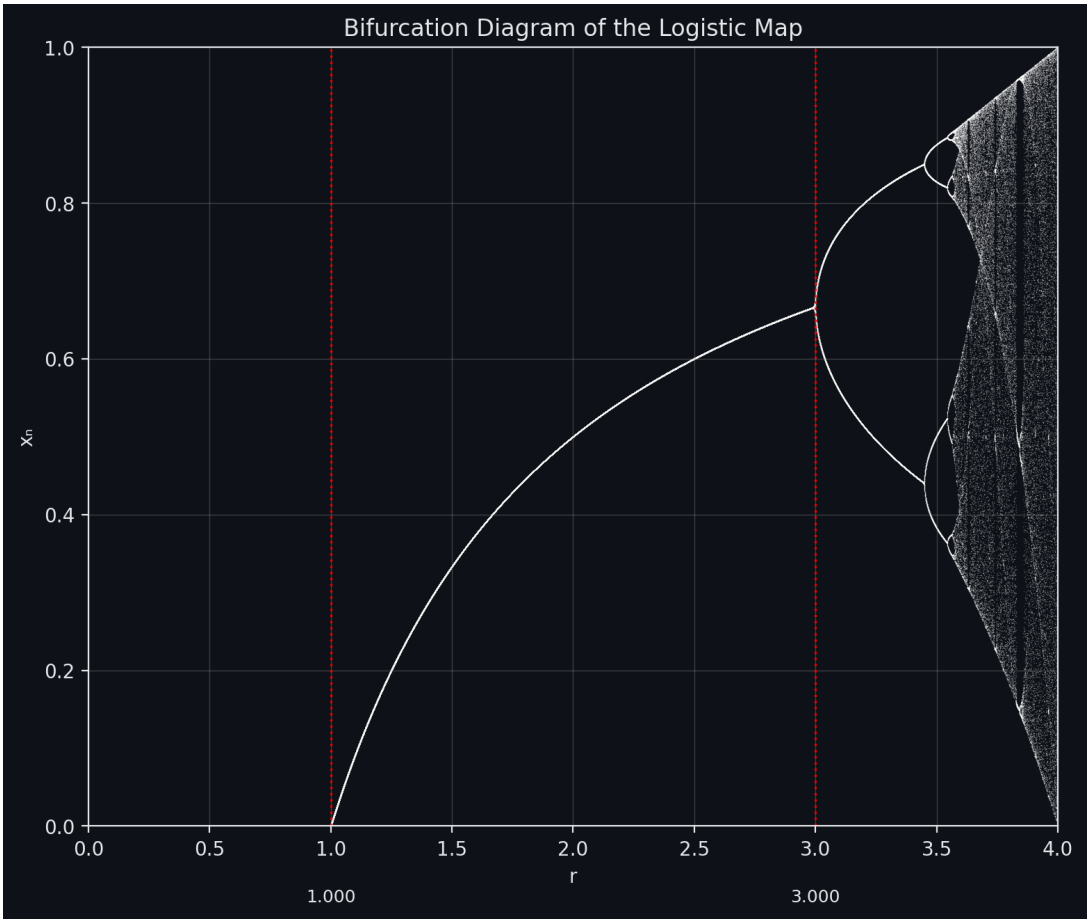

Figure 3: Bifurcation diagram of the logistic map for $1 < r < 3$, showing the period-1 stability window. From: Author's own visualisation [7]

In Fig.3, it can be observed that when $r \in]1, 3[$ the recurrence application settles to one value; therefore, we call this region a period-1 window.

This periodicity translates, in population dynamics, to the population oscillating between n values as seen in Fig. 4: (a), (b), (c) and (d).

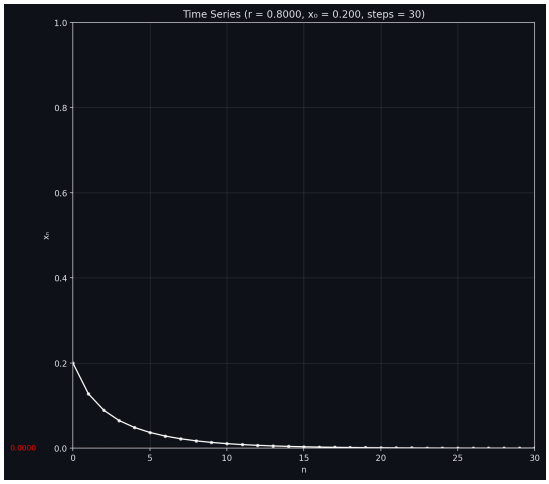

(a) $r = 0.8$, $x_0 = 0.2$ (extinguishing cycle).

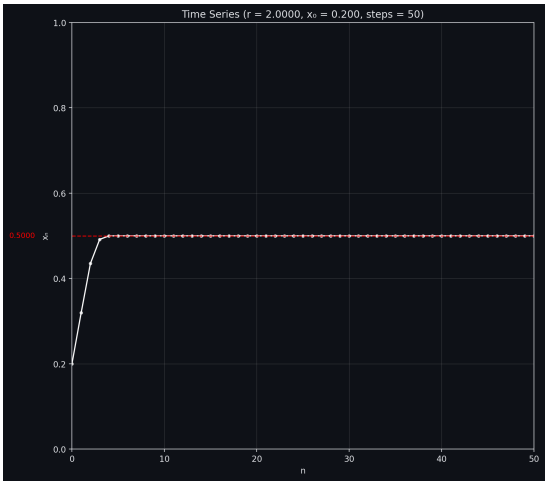

(b) $r = 2.0$, $x_0 = 0.2$ (1-periodic cycle).

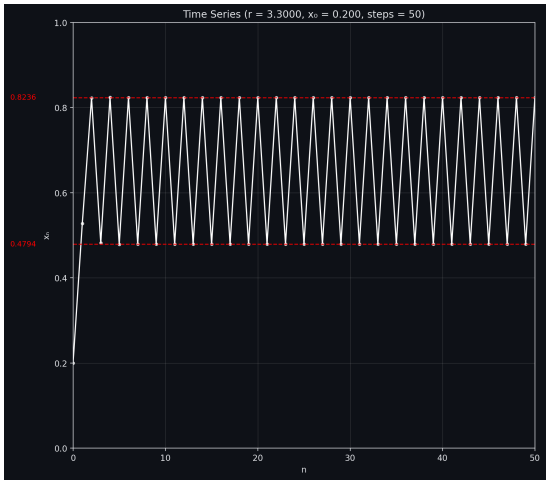

(c) $r = 3.3$, $x_0 = 0.2$ (2-periodic cycle).

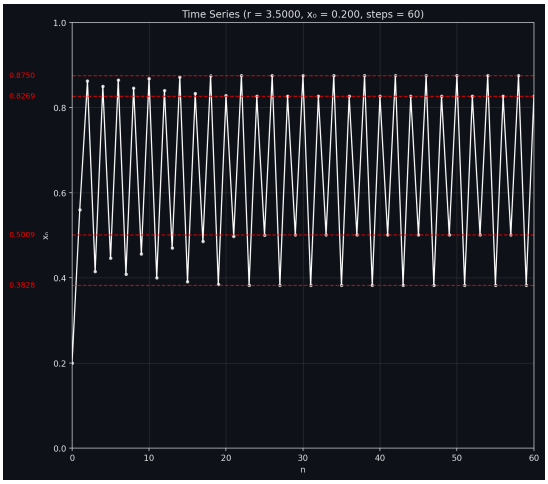

(d) $r = 3.5$, $x_0 = 0.2$ (4-periodic cycle).

Figure 4: Time series plots of the logistic map for different parameter values r, starting from $x_0 = 0.2$. Each trajectory x_n converges to a stable periodic orbit, illustrated by red dashed lines indicating the attracting cycle values. Panel (a) shows the population extinguishing after a certain number of steps, (b) shows the population converging to a fixed point (1-periodic cycles), while (c) and (d) show the population converging to higher-order periodic cycles (2-periodic and 4-periodic respectively). From: Author's own visualisation [7].

2.2.3 Period-doubling and the bifurcation diagram

When the growth rate parameter r is increased beyond $r = 3$, the fixed point

$$x_1^* = 1 - \frac{1}{r}$$

loses stability [22]. This is because at $r = 3$, we have

$$x_1^* = \frac{2}{3}$$

$$\therefore |f_r'(x_1^*)| = 1$$

This indicates the beginning of a bifurcation; rather than converging to a single value, the population oscillates between two distinct values, therefore, the region following $r = 3$ is a period-2 region. This is the first example of a period-doubling bifurcation, where the system's attractor changes from period k to period $2k$. [23] [24] [25]

Definition: A *periodic attractor* is the set of values towards which a system tends to approach after many iterations, regardless of the initial conditions. In the context of the logistic map, the attractor can be a single fixed point, a finite cycle of period n, or, for larger values of r, a chaotic set [26] [27]. The attractor therefore represents the long-term behaviour of the system.

The logistic map creates the following bifurcations as r increases:

1. At $r = 3.000$, the stable period-1 point bifurcates to period-2 (2.2.4) (see Fig.5).
2. At $r = 1 + \sqrt{6} \approx 3.449$, the period-2 cycle bifurcates to period-4 (2.2.4) (see Fig.6).
3. The following period doublings, happen more and more rapidly after period-2. The intervals between bifurcation values shrink geometrically as r converges to the **Feigenbaum point** [28]

   $$r_\infty \approx 3.569946\ldots,$$

   beyond which the system enters chaos [29] [30].

The ratio of successive differences in bifurcation parameters,

$$\delta \;=\; \lim_{n\to\infty} \frac{r_n - r_{n-1}}{r_{n+1} - r_n},$$

is a universal constant ($\delta \approx 4.6692$) [25], independent of the specific form of the quadratic map. This universality links the logistic map to other nonlinear dynamical systems, including the quadratic polynomial $f_c(z) = z^2 + c$ underlying the Mandelbrot set [31] [32].

Stability windows appear as horizontal bands containing a finite set of points (periodic attractors). The period-n windows of the bifurcation diagram have a direct relation to the period-n bulbs of the Mandelbrot set as will be shown in 4.1.

2.2.4 Example calculations for small periods

The values of r that generate k-periodic cycles (with prime periods k, $k > 1$) of the logistic map as r goes beyond 3 can be found when solving for r [33]:

$$f_r^{(k)}(x^*) = x^*, \quad f_r(x^*) \neq x^*. \tag{8}$$

A cycle is said to have prime period k if k is the smallest positive integer such that

$$f_r^{(k)}(x^*) = x^*,$$

while no smaller $(m < k) \in \mathbb{N}$ satisfies $f_r^{(m)}(x^*) = x^*$. In other words, a prime period-k cycle consists of k distinct points visited in order by the map, and the orbit does not close up after fewer than k iterations [34].

Period-2 cycle. A point x^* belongs to a period-2 cycle (has a prime period of $k = 2$) if it satisfies:

$$f_r^{(2)}(x^*) = f_r(f_r(x^*)) = x^*, \quad f_r(x^*) \neq x^*.$$

Expanding

$$f_r(x) = rx(1-x),$$

$$f_r^{(2)}(x) = f_r(rx(1-x)) = r\big(rx(1-x)\big)\Big(1 - rx(1-x)\Big).$$

So the equation becomes

$$r^2x(1-x)(1-rx+rx^2) = x.$$

Rearranging gives a cubic equation whose solutions include; the fixed points (period-1), and two others which correspond to the period-2 orbit. Solving explicitly gives:

$$x_{1,2} = \frac{r + 1 \pm \sqrt{(r-3)(r+1)}}{2r}.$$

This pair is stable when

$$\left|(f_r^{(2)})'(x^*)\right| < 1,$$

which holds for $3 < r < 1 + \sqrt{6} \approx 3.449$. This interval corresponds to the period-2 stability window observed in the bifurcation diagram (see Fig.5).

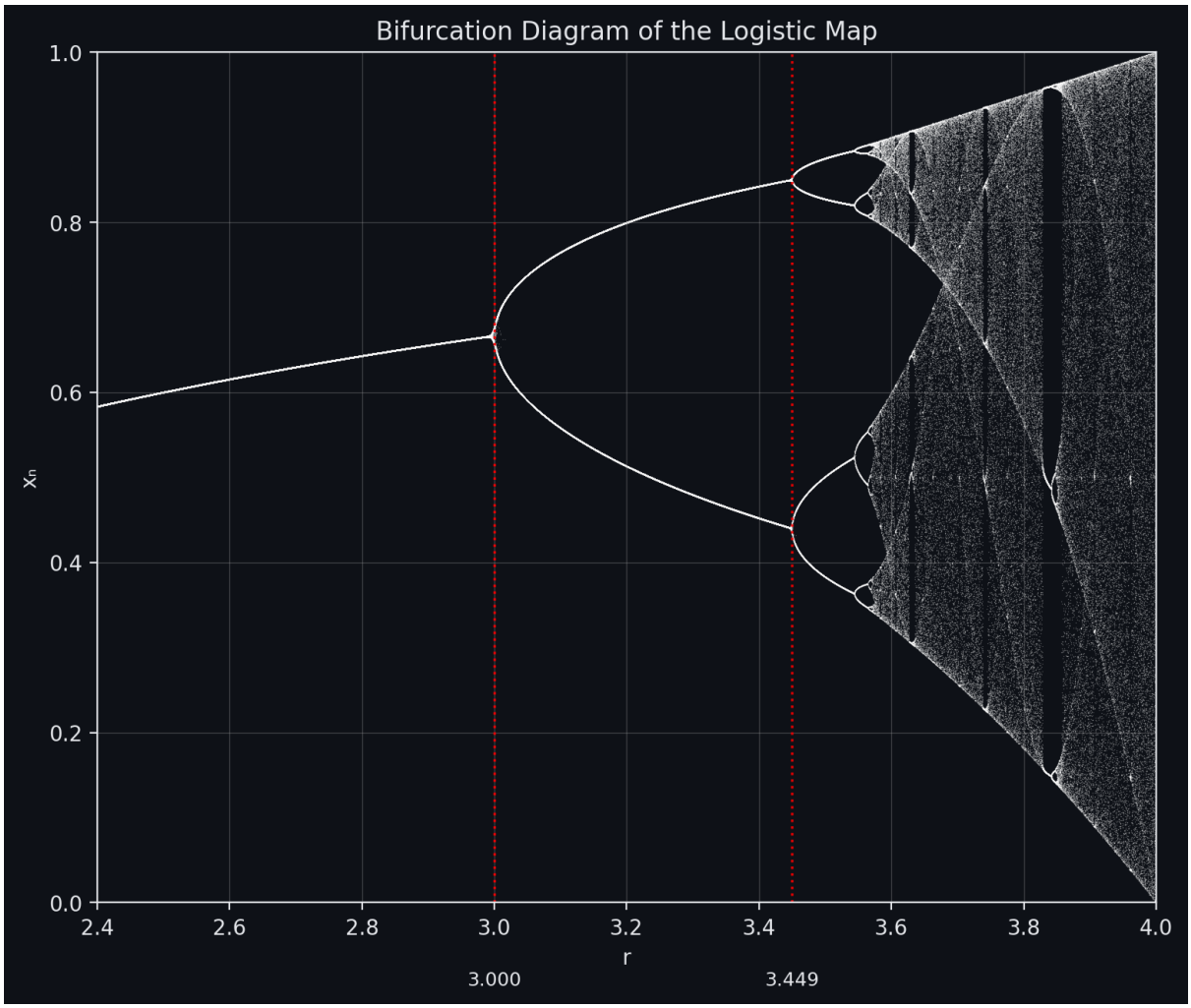

Figure 5: Bifurcation diagram of the logistic map for $3 < r < 1 + \sqrt{6}$, showing the period-2 stability window. From: Author's own visualisation [7]

Period-4 cycle. Similarly, a period-4 point satisfies

$$f_r^{(4)}(x^*) = x^*, \quad f_r^{(k)}(x^*) \neq x^* \text{ for } k < 4.$$

To evaluate solutions (x^*) for this expression, let us first write the 2-iteration function:

$$g(x) = f_r^{(2)}(x) = r^2 x(1-x)(1 - rx + rx^2).$$

Therefore, a point has period 4 if

$$g^{(2)}(x^*) = x^*,$$

but $g(x^*) \neq x^*$ (not period 2) and $f_r(x^*) \neq x^*$ (not period 1).

The equation $g(g(x)) - x = 0$ expands to a polynomial of degree 16. We can simplify it by noting that some solutions correspond to period-1 and period-2 cycles, and factoring them out, the remaining roots give the period-4 cycle. The exact algebraic expressions are extremely complicated [35], so we do not write them here.

Stability. A 4-cycle $\{x_0, x_1, x_2, x_3\}$ is stable when

$$\left|(f_r^{(4)})'(x_0)\right| < 1.$$

We know,

$$f_r(x) = r\,x(1-x) \text{ and } x_{j+1} = f_r(x_j), \quad j = 0, 1, 2, 3, \quad (x_4 = x_0).$$

$$\begin{aligned}
\therefore (f_r^{(2)})'(x_0) &= (f_r \circ f_r)'(x_0) = f_r'\big(f_r(x_0)\big) \cdot f_r'(x_0) = f_r'(x_1)\, f_r'(x_0), \\
\therefore (f_r^{(3)})'(x_0) &= \big(f_r \circ f_r^{(2)}\big)'(x_0) = f_r'\big(f_r^{(2)}(x_0)\big) \cdot (f_r^{(2)})'(x_0) = f_r'(x_2)\,\big[f_r'(x_1)\, f_r'(x_0)\big], \\
\therefore (f_r^{(4)})'(x_0) &= \big(f_r \circ f_r^{(3)}\big)'(x_0) = f_r'\big(f_r^{(3)}(x_0)\big) \cdot (f_r^{(3)})'(x_0) \\
&= f_r'(x_3)\,\big[f_r'(x_2)\, f_r'(x_1)\, f_r'(x_0)\big] \\
&= \prod_{j=0}^{3} f_r'(x_j).
\end{aligned}$$

Taking absolute values,

$$\left|(f_r^{(4)})'(x_0)\right| \;=\; \prod_{j=0}^{3} \left|f_r'(x_j)\right|.$$

Since $f_r'(x) = r(1-2x)$, this becomes

$$\left|(f_r^{(4)})'(x_0)\right| \;=\; \prod_{j=0}^{3} \big|\, r(1-2x_j)\,\big| \;=\; |r|^4 \prod_{j=0}^{3} \left|1-2x_j\right| < 1 \tag{9}$$

We call this stability condition the *multiplier condition* [36], we often denote it $|\Lambda| < 1$.

This condition gives the range of r values where a 4-cycle appears. The 4-cycle first appears exactly when the period-2 cycle becomes unstable, which happens at

$$r = 1 + \sqrt{6} \approx 3.449.$$

It remains stable until the next bifurcation at

$$r \approx 3.544.$$

Therefore, the period-4 cycle exists and is stable for

$$\boxed{3.449 < r < 3.544}.$$

Within this interval [37], the logistic map cycles between 4 point as observed on the bifurcation diagram (see Fig.6).

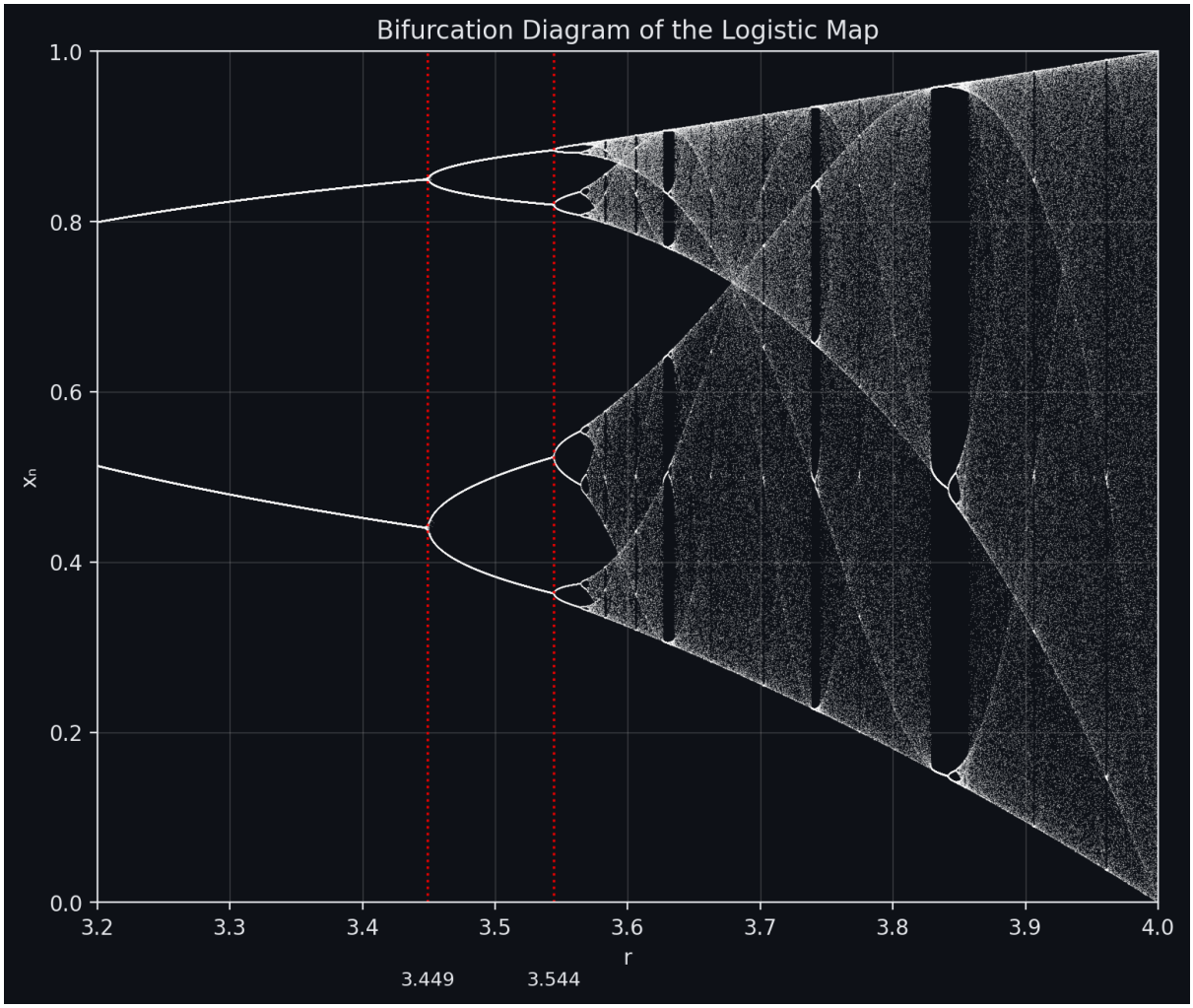

Figure 6: Bifurcation diagram of the logistic map for $3.449 < r < 3.544$, showing the period-4 stability window. From: Author's own visualisation [7], 2025.

The same process can be followed for larger k-periodic cycles.

The main limitation of the multiplier condition is that it only detects local stability. At bifurcation points, where the multiplier equals ± 1 [38], convergence of the orbits towards the cycle becomes arbitrarily slower, making stability harder to determine numerically [39]. This becomes a particularly relevant problem when computing stability for higher values of k. Making it harder to link the bifurcation structure of the logistic map to the bulbs in the Mandelbrot set.

3 Methodology

3.1 Hypotheses

The following hypothesis about the relationship between the period-n bulbs and stability windows of the logistic map will be used to drive this essay.

Null hypothesis. There is no systematic correspondence between the period-n bulbs of the Mandelbrot set and the stability windows of the logistic map; any resemblance is accidental.

Research hypothesis. The period-n bulbs of the Mandelbrot set correspond directly to the period-n stability windows of the logistic map, such that each bulb predicts a parameter interval of stable cycles in the bifurcation diagram.

3.2 Analytical approach

Deriving conjugacy is appropriate in this investigation as conjugacy allows us to preserve properties of one system to the other; periodicity and multipliers, for example, which help us determine whether the two systems are really related or not. This is because these quantities determine the location of stability regions in the logistic map and the structure of bulbs in the Mandelbrot set. Conjugacy, therefore, provides a rigorous framework for transferring analytical results about both the cycles, and the centres and boundaries between the two families.

3.3 Numerical approach

Calculating stability intervals, centres, and endpoints in the logistic map, and mapping them through to the quadratic family, allows me to confirm the results found in the analysis part and will help me address the research hypothesis. The calculations will consist of 2 main checks:

Interval mapping. For each period-k stability window of the logistic map, the multiplier condition $|(f_r^k)'(x^*)| < 1$ is applied to determine the stability interval in r. These intervals are then mapped through the conjugacy found to identify the corresponding slices of the Mandelbrot set. Similarly, window endpoints where $|(f_r^k)'(x^*)| = 1$ are mapped to parabolic points on the boundary of the corresponding bulb.

Centre mapping. Centres are found by solving $f_r^k(\frac{1}{2}) = \frac{1}{2}$ for prime periods k, and verified against $P_c^k(0) = 0$ to confirm the correspondence of superattracting centres.

I will independently compute the centres and endpoints of the stability windows and map them between the two families, verifying the alignment.

Limitations. Numerical detection loses precision as the multiplier ($|\Lambda|$) tends to 1, where stability changes occur; therefore, endpoints are reported with a set precision of $\pm 10^{-5}$.

3.4 Computational approach

Alongside the Numerical approach, exploring the systems visually and through a computer, can help confirm certain results. I therefore developed two interactive Python programs to visualise and experiment with both the Mandelbrot set and the logistic map: a logistic map explorer and a Mandelbrot explorer. The visualisations of this essay are generated through these explorers.

Screenshots of both interfaces are provided in the Appendices (4.4), the GitHub repository, containing the full code, is also linked. These computational tools extend the investigation helping to get a feel of the behaviour of both families by producing accurate diagrams and visualisations of their structures, helping us to get a more concrete understanding of the mathematics at play (rather than being purely theoretical).

4 Analysis

4.1 Connection between Logistic Map and Mandelbrot Set

4.1.1 Definitions

Maps.

Let X be a set (in this essay, $X \subseteq \mathbb{R}$ or $X \subseteq \mathbb{C}$). A *map* is a rule $f : X \to X$ that assigns to each $x \in X$ a value $f(x) \in X$ [40].

Conjugacy.

A *conjugacy* between two dynamical systems implies essentially equivalent systems under a change of coordinates. We define it as follows:

Let $f : X \to X$ and $g : Y \to Y$ be maps. We say that f and g are *conjugate* if there exists an invertible change of coordinates $h : X \to Y$ (a bijection, i.e. a one-to-one and onto correspondence) such that [41]

$$h \circ f = g \circ h.$$

If h is affine (linear plus shift), we say f and g are *affinely conjugate* [42]. Conjugacy preserves the structure of the dynamics, in particular the existence, period, and stability of cycles. This makes it possible to transfer results from one system to another [43]. Therefore, proving conjugacy between the logistic map and the Mandelbrot set will be crucial in demonstrating the link between the hyperbolic components of the Mandelbrot set and the logistic map.

Superattraction.

A cycle is called "superattracting" if and only if it contains a critical point $z = 0$, making the multiplier

$$\left|(f_r^{(4)})'(x_0)\right| \;=\; \prod_{j=0}^{3} \left| r(1-2x_j) \right| \;=\; |r|^4 \prod_{j=0}^{3} |1-2x_j| = 0$$

Therefore, forcing convergence to the k-periodic cycle [44].

Critical points.

For a differentiable map $f(x)$, a *critical point* is a value x_c where the derivative:

$$f'(x_c) = 0.$$

The *critical orbit* is the sequence $\{f^n(x_c)\}_{n\geq 0}$. In one-dimensional iterative maps, the orbit of the critical point is decisive because if it converges to a cycle, that cycle is attracting [45].

Centre.

The *centre* of a hyperbolic component of the Mandelbrot set is the parameter value c for which the associated attracting cycle is superattracting. [10]

4.1.2 Criteria for conjugacy

Looking at the connection between the logistic map and the Mandelbrot set will be done through showing conjugacy between the two systems.

We now introduce two parallel criteria that allow a rigorous comparison between the logistic map and the quadratic family:

- For the logistic family $f_r(x) = r\,x(1-x)$, a *period-k stability window* is an r-interval on which there exists an attracting cycle of prime period k. Such a cycle is found by the periodic-point equation

$$f_r^{(k)}(x^*) = x^* \quad \text{(with prime period } k\text{)},$$

and the *multiplier* (stability) condition

$$\left|(f_r^{(k)})'(x^*)\right| = \prod_{j=0}^{k-1} \left|f_r'(x_j)\right| = \prod_{j=0}^{k-1} \left|r(1-2x_j)\right| < 1,$$

where $x_{j+1} = f_r(x_j)$ along the cycle.

- For the quadratic family $P_c(z) = z^2 + c$, a *period-n bulb* (hyperbolic component) consists of the parameters c for which there exists an attracting n-cycle. The *centre* of the bulb is characterised by a *superattracting* n-cycle,

$$P_c^{(n)}(x^*) = 0 \quad \text{and} \quad P_c^{(m)}(x^*) \neq 0 \text{ for } m < n.$$

The criteria above establish a rigorous bridge between the two systems by showing a conjugacy between the two (see 4.1.3). By constructing a parameter map and an affine conjugacy, we can transfer period and stability information directly from the logistic map to the quadratic family, thereby explaining the correspondence between period-n stability windows of the logistic map and the period-n bulbs of the Mandelbrot set. In this essay, the connection between the logistic map and the quadratic family is restricted to real parameters due to the way the logistic map is defined ($r \in \mathbb{R}$). However, the Mandelbrot set is defined over the full complex plane, so the correspondence we obtain is exact only along the real slice. Expanding this link over the complex numbers can however be done, providing a fascinating extension to this essay.

4.1.3 A parameter conjugacy linking f_r and P_c.

Analytical demonstration of conjugacy.

For each fixed $r \in \mathbb{R}$, define the affine maps

$$T(x) = 1 - 2x, \qquad S_r(y) = \tfrac{r}{2}y, \qquad \Phi_r = S_r \circ T.$$

We can attempt to transform the logistic map into a quadratic family to create a conjugacy.

Starting from $f_r(x) = rx(1-x)$, we compute

$$\begin{aligned} T\big(f_r(x)\big) &= 1 - 2rx(1-x) \\ &= 1 - \tfrac{r}{2}\big(1 - T(x)^2\big) \\ &= \tfrac{r}{2}T(x)^2 + \Big(1 - \tfrac{r}{2}\Big). \end{aligned}$$

Applying S_r gives

$$\begin{aligned} \Phi_r\big(f_r(x)\big) &= S_r\big(\tfrac{r}{2}T(x)^2 + 1 - \tfrac{r}{2}\big) \\ &= \big(S_r(T(x))\big)^2 \; + \; \tfrac{r}{2}\Big(1 - \tfrac{r}{2}\Big). \end{aligned}$$

A quadratic family has emerged under a transformation of r that we define

$$\psi(r) = \frac{r(2-r)}{4}.$$

The previous identity becomes

$$\Phi_r \circ f_r(x) \;=\; \big(\Phi_r(x)\big)^2 + \psi(r).$$

We therefore obtain the affine conjugacy

$$\boxed{\Phi_r \circ f_r = P_{\psi(r)} \circ \Phi_r} \qquad \text{with} \qquad P_c(z) = z^2 + c.$$

Hence, for each fixed r, the logistic map f_r is affinely conjugate to the quadratic polynomial $P_{\psi(r)}$ under the change of variables Φ_r. Note that this conjugacy only relates the *real slice* of the parameter space, since $\psi(r) \in \mathbb{R}$. Phenomena involving complex parameters $c \notin \mathbb{R}$ lie beyond this correspondence.

Consequences.

Let x^* be a prime period-k point of f_r and $z^* = \Phi_r(x^*)$. Then

$$\Phi_r\big(f_r^{(k)}(x^*)\big) = \Phi_r(x^*) \quad \Longleftrightarrow \quad P_{\psi(r)}^{(k)}(z^*) = z^*,$$

so z^* is a period-k point for $P_{\psi(r)}$. Moreover, differentiating the conjugacy $\Phi_r \circ f_r^{(k)} = P_{\psi(r)}^{(k)} \circ \Phi_r$ and using that Φ_r is affine (constant nonzero derivative) gives

$$(P_{\psi(r)}^{(k)})'(z^*) = (f_r^{(k)})'(x^*).$$

Hence multipliers are identical: a cycle is attracting/neutral/repelling for f_r if and only if the corresponding cycle is so for $P_{\psi(r)}$. Hence it can be said that the stability of both systems is equal. However equality of multipliers does not imply equality of geometric shape of attractors, only their local stability type. Therefore:

> For each k, the set of parameters r for which f_r has an attracting period-k cycle maps under $c = \psi(r)$ onto the set of parameters c for which P_c has an attracting period-k cycle. In particular, each logistic stability window of period k corresponds to a period-k bulb of the Mandelbrot set (restricted to the real slice of parameter space via $c = \psi(r)$).

Limitation. The correspondence between period-k windows and period-k bulbs holds along the real slice $c = \psi(r)$, but it does not describe the full structure of the Mandelbrot set. Each period-k bulb is organised around a superattracting k-cycle at its centre, yet its interior also contains further bifurcations $k \to 2k \to 4k \to \cdots$ and other dynamics that are not visible from the one-dimensional logistic bifurcation diagram. This is seen in Fig.7 where hyperbolic components of doubling period are seen outside of the real slice (where the imaginary component of c satisfies $\Im(c) \neq 0$).

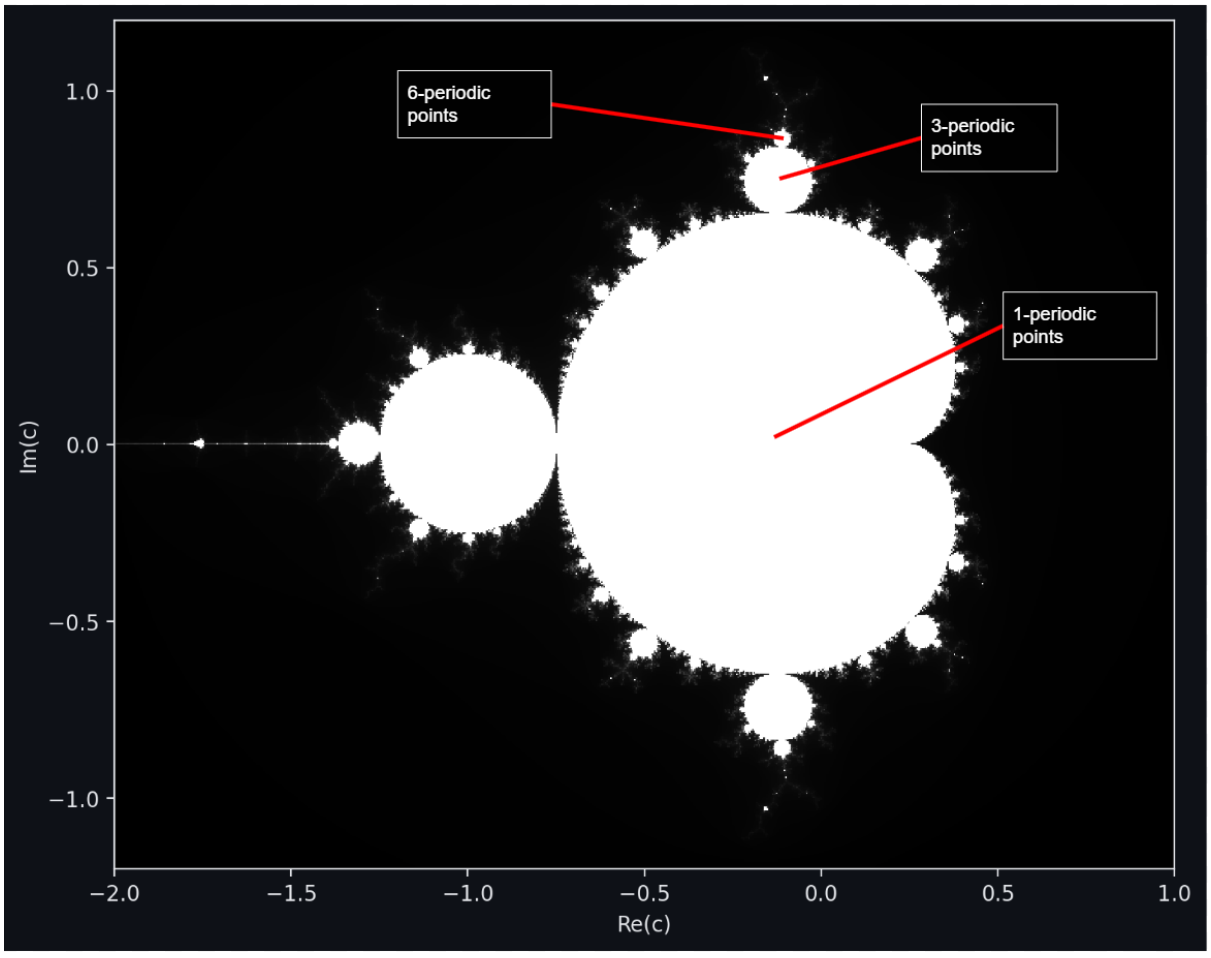

Figure 7: Annotated Mandelbrot set showing bulbs of different periodicity, with examples of 1-, 3-, and 6-periodic points indicated. From: Author's own visualisation [7]

This limitation is much clearer in the following image by Adam Cunningham (see Fig.8).

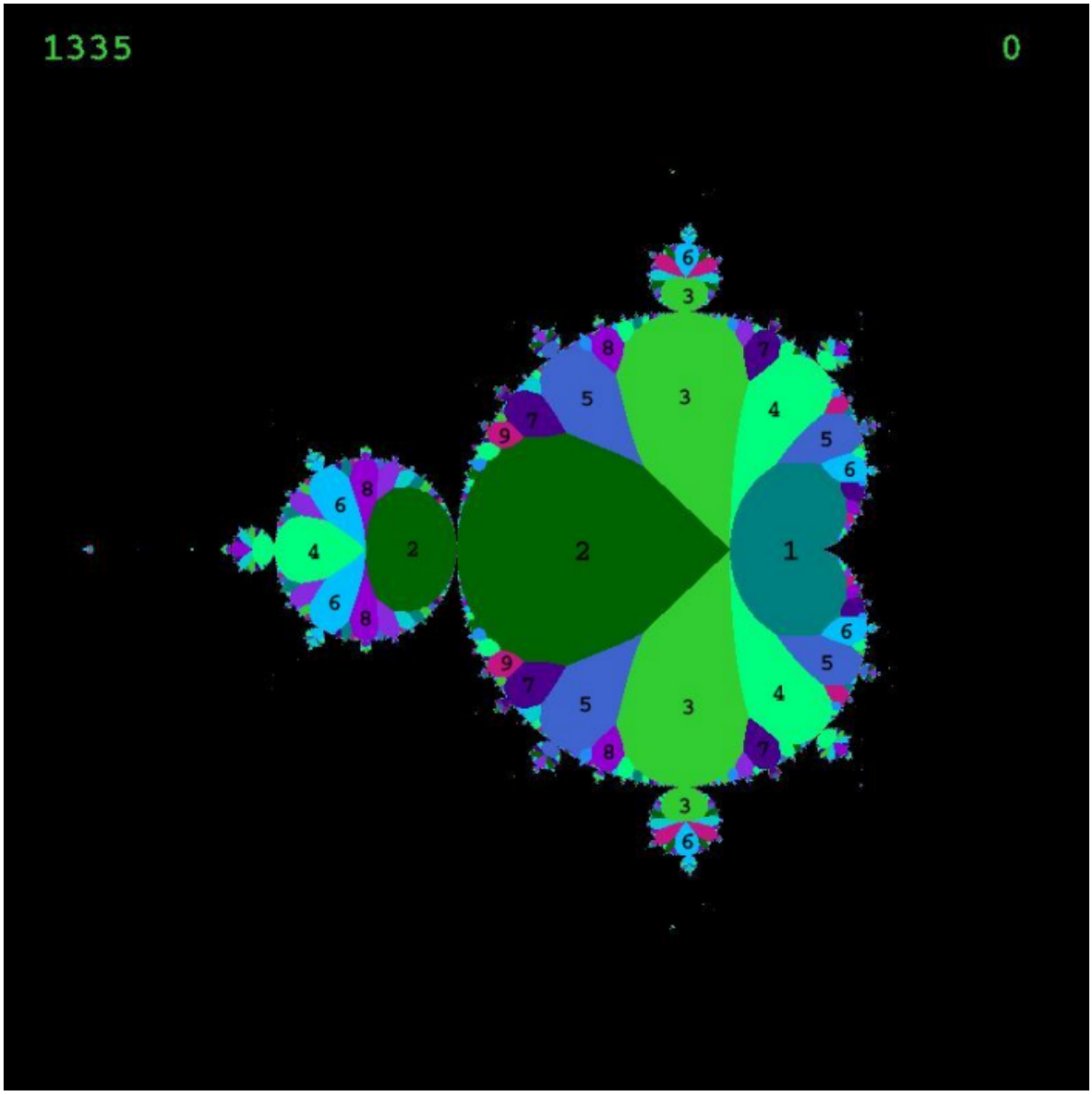

Figure 8: Orbit cycle map of the Mandelbrot set, showing the internal partition of the set into distinct hyperbolic components labelled by the period of the attracting cycle. Each coloured region corresponds to parameters c for which P_c converges to a cycle of the labelled period. From: Cunningham, A. (2013), *Displaying the Internal Structure of the Mandelbrot Set*, State University of New York at Buffalo. [46]

It was shown by Douady and Hubbard (1985) [47] that the Mandelbrot set contains hyperbolic components of every period n. Crucially, most of these lie in the complex plane rather than on the real slice considered here. This highlights that the correspondence established in this essay captures only a restricted view. Extending the analysis to complex parameters would open doors to higher-order dynamics and concepts such as internal bifurcations, richer fractal substructures, and perhaps more interesting results.

Moreover, away from the real axis, the boundaries of these bulbs are surrounded by disconnected bulbs, referred to as satellite bulbs and are essentially smaller Mandelbrot sets (see Fig.9), as well as other bulbs with varied internal angles. Thus, the period-k label captures the real-slice correspondence but not the other fractal substructures off the real line.

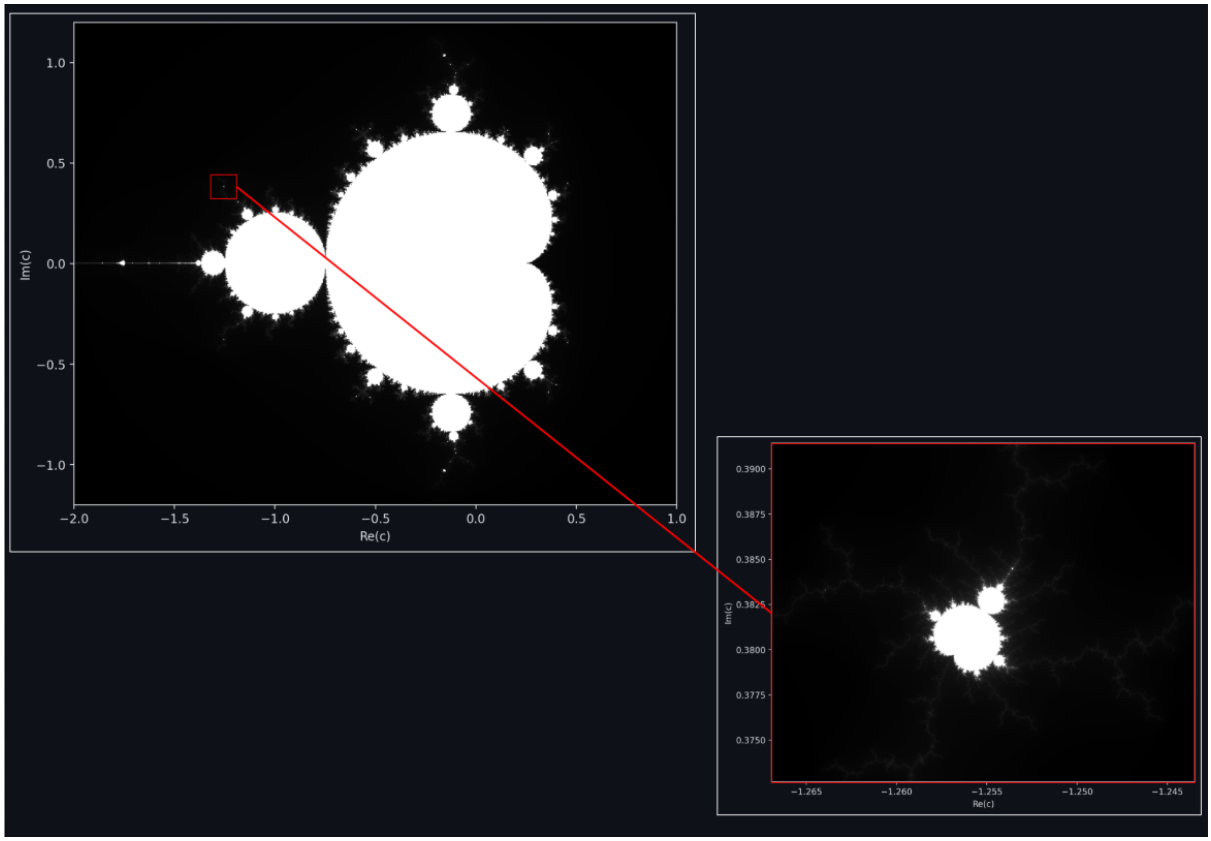

Figure 9: Zoom into a satellite copy of the Mandelbrot set. The left panel shows the full set with the selected region marked in red, while the right panel illustrates the magnified satellite structure, which replicates the overall form of the Mandelbrot set. From: Author's own visualisation [7]

4.2 Numerical Correspondences and Calculations

To confirm the results obtained in 4.1.3, we now compute the exact transforms for the first stability windows and their corresponding bulbs, verifying that their boundaries and centres coincide. Throughout these calculations we restrict attention to the real slice of the Mandelbrot set; accordingly, references to 'cardioids' or other hyperbolic components of the Mandelbrot set are to be interpreted as referring only to their intersections with the real axis.

4.2.1 Period-1

Stability window mapping.

The nonzero fixed point of f_r is $x^* = 1 - \frac{1}{r}$ with multiplier

$$f_r'(x^*) = r(1 - 2x^*) = r\Big(1 - 2 + \tfrac{2}{r}\Big) = 2 - r.$$

Similarly, the fixed points of P_c are solutions of

$$z^* = (z^*)^2 + c.$$

For such a fixed point, the multiplier is

$$(P_c)'(z^*) = 2z^* = 2 \cdot \frac{1 \pm \sqrt{1 - 4c}}{2} = 1 \pm \sqrt{1 - 4c}.$$

The stability condition $|2 - r| < 1$ gives $1 < r < 3$. Under the mapping $c = \psi(r) = \frac{r(2-r)}{4}$, the endpoints map to

$$r = 1 \;\mapsto\; c = \tfrac{1}{4}, \qquad r = 3 \;\mapsto\; c = -\tfrac{3}{4}.$$

At the right endpoint $c = \frac{1}{4}$ the fixed point becomes neutral with multiplier $+1$; at the left endpoint $c = -\frac{3}{4}$ the multiplier is -1. The mapped endpoints are therefore precisely the endpoints of the real slice of the main cardioid ($c \in (-\frac{3}{4}, \frac{1}{4})$).

Centre mapping.

The superattracting fixed point for f_r occurs when $f_r(\frac{1}{2}) = \frac{1}{2}$, i.e.

$$\frac{r}{4} = \frac{1}{2} \implies r = 2, \qquad c = \psi(2) = 0.$$

This, $c = 0$ being the centre of the main cardioid ($P_0(z_n) = 0,$ with $z_0 = 0$), confirms a centre-to-centre correspondence over the first periodicity window.

4.2.2 Period-2

Stability window mapping.

A period-2 window begins when the period-1 fixed point loses stability: $r = 3 \mapsto c = -\frac{3}{4}$. The period-2 window persists until the period-2 cycle becomes neutral ($r = 1 + \sqrt{6}$), mapping under ψ gives

$$r = 1 + \sqrt{6} \;\mapsto\; c = \psi(1 + \sqrt{6}) = \frac{(1 + \sqrt{6})(2 - (1 + \sqrt{6}))}{4} = -\frac{5}{4}.$$

Thus the real slice of the period-2 bulb is the window $c \in (-\frac{5}{4}, -\frac{3}{4})$, matching the known window for the period-2 bulb [48].

Centre mapping.

Solve $f_r^{(2)}(\frac{1}{2}) = \frac{1}{2}$ with $f_r(\frac{1}{2}) \neq \frac{1}{2}$:

$$f_r\Big(\tfrac{1}{2}\Big) = \frac{r}{4}, \qquad f_r^{(2)}\Big(\tfrac{1}{2}\Big) = r \cdot \frac{r}{4}\Big(1 - \frac{r}{4}\Big) = \frac{r^2}{4}\Big(1 - \frac{r}{4}\Big).$$

Set $f_r^{(2)}(\frac{1}{2}) = \frac{1}{2}$:

$$\frac{r^2}{4}\Big(1 - \frac{r}{4}\Big) = \frac{1}{2} \quad \Longleftrightarrow \quad 4r^2 - r^3 - 8 = 0 \quad \Longleftrightarrow \quad (r - 2)(r^2 - 2r - 4) = 0.$$

Reject $r = 2$ (period 1). Hence $r = 1 + \sqrt{5} \approx 3.23607$, and

$$c = \psi(1 + \sqrt{5}) = \frac{(1 + \sqrt{5})(2 - (1 + \sqrt{5}))}{4} = \frac{(1 + \sqrt{5})(1 - \sqrt{5})}{4} = \frac{1 - 5}{4} = -1,$$

the centre of the 2-periodic bulb. As expected, the cycle includes $x = \frac{1}{2}$, so the multiplier is 0. Therefore a centre-to-centre mapping can also be done here.

4.2.3 Mapping table.

The same process can be followed for further periods and the results found are as follows (to 5 s.f.):

Period	Logistic window in r	centre r	Image in $c = \psi(r)$ (real slice)
1	$1 < r < 3$	$r = 2$	$-\frac{3}{4} < c < \frac{1}{4}$, centre $c = 0$
2	$3 < r < 1 + \sqrt{6}$	$r = 1 + \sqrt{5}$	$-\frac{5}{4} < c < -\frac{3}{4}$, centre $c = -1$
4	$1 + \sqrt{6} < r \lesssim 3.54409$	$r \approx 3.49856$	$-1.36810 \lesssim c < -\frac{5}{4}$, centre $c \approx -1.31070$
8	$3.54408 \lesssim r \lesssim 3.56428$	$r \approx 3.55464$	$-1.39389 \lesssim c < -1.36809$, centre $c \approx -1.38155$
16	$3.56428 \lesssim r \lesssim 3.56871$	$r \approx 3.56667$	$-1.39957 \lesssim c < -1.39389$, centre $c \approx -1.39695$
...	...	...	...

4.3 Scope, assumptions, and limitations

(i) Local stability: The multiplier test ($|\Lambda| < 1$, with Λ being the multiplier) is a criterion for stability that only works in the very local neighbourhood of a cycle. Near the boundary (when $|\Lambda| = 1$), convergence becomes arbitrarily slow and orbits become extremely long before stabilising, making the stability harder to notice numerically. Since finite-precision as well as finite iteration depth are used, it causes an attracting cycle to appear unstable. These difficulties increase for higher-period cycles and when attempting to find bifurcation points with high precision.

(ii) Prime-period detection: When solving $f_r^{(k)}(x) = x$ algebraically, the equation also admits solutions corresponding to lower-period cycles that divide k. For example, when solving for the cycle of prime period 8, we get solutions of the period-2 and period-4 cycles. Without additional checks, this would lead to false positives of prime period k while the orbit is of lower periodicity. To address this, one usually factors out lower period factors and solve for the remaining ones. numerical period tests can also be applied to confirm that the prime period of the orbit is k. This method, while useful, is computationally more expensive for larger k and does not completely eliminate sensitivity at boundary points. Therefore, prime-period cycles near bifurcation points or near boundaries of hyperbolic components remain approximate.

(iii) Measure-zero exceptions: Certain parameter values, such as Misiurewicz points [49] where the critical orbit is periodic, do not fall inside stability windows but instead lie on their boundaries or within chaotic regions. These points form sets of measure zero, meaning they occupy no interval in parameter space and do not affect the correspondence between windows and bulbs. Nevertheless, they introduce local irregularities as, near such parameters, cycles can appear to destabilise, and numerical tests become less reliable. Their existence highlights that the connection between stability windows and hyperbolic components is only exact at the level of attracting cycles. In order to link their boundaries as well as their chaotic areas requires more advanced tools beyond the scope of this essay.

4.4 Conclusion

The ivestigation above establishes four courrespondences on the real parameter slice:

1. **Parameter map and conjugacy.** I derived an explicit parameter transformation

   $$c = \psi(r) = \tfrac{r(2-r)}{4},$$

   as well as an affine conjugacy Φ_r such that $\Phi_r \circ f_r = P_c \circ \Phi_r$. Therefore showing that the logistic family and the quadratic family are dynamically equivalent along the real parameter slice.

2. **Preservation of stability.** Because Φ_r is affine, multipliers of corresponding cycles are equal. This means that attracting, neutral, and repelling behaviour in the logistic map transfers to equal behaviour in the quadratic family. Thus the classification of stability windows in r is equivalent to the classification of hyperbolic components in c.

3. **Critical orbit and centres.** The logistic critical point $x = \frac{1}{2}$ maps directly to $z = 0$ (the critical point of P_c). Since superattracting cycles contain the critical orbit, the condition $f_r^{(n)}(\frac{1}{2}) = \frac{1}{2}$ corresponds to $P_c^{(n)}(0) = 0$. Hence the centres of logistic stability windows map to the centres of the Mandelbrot bulbs. This was confirmed in our computations for periods 1, 2, 4, 8, and 16.

4. **Boundaries of windows and bulbs.** The boundaries of stability windows occur where the multiplier has modulus one: $|(f_r^{(k)})'(x^*)| = 1$ or equivalently $|(P_c^{(k)})'(z^*)| = 1$. Under the parameter map, the logistic bifurcation thresholds align with the boundary points of the Mandelbrot bulbs. Therefore, we can conclude that the endpoints of stability windows correspond across the two systems.

Therefore, it can be concluded that, on the real slice, the period-n stability windows of the logistic map correspond, under $c = \psi(r)$, to the period-n bulbs of the Mandelbrot set, confirming the research hypothesis, and thus rejecting the null hypothesis. The correspondence is exact on the real slice and at the level of periods/multipliers. However, the different geometric structures outside the real axis require complex analytical tools, making a great extension to this essay.

References

[1] Fractal Foundation, "What Are Fractals?" https://fractalfoundation.org/resources/what-are-fractals/, accessed: 2025-08-17.

[2] K. Falconer, *Fractals: A Very Short Introduction*. Oxford: Oxford University Press, 2013.

[3] J. C. P. Campuzano and B. S. Chongchitmate, "5.5: The Mandelbrot Set," Mathematics LibreTexts, 2025, accessed: 2025-08-17. [Online]. Available: https://math.libretexts.org/Bookshelves/Analysis/Complex_Analysis_-_A_Visual_and_Interactive_Introduction_(Ponce_Campuzano)/05%3A_Chapter_5/5.05%3A_The_Mandelbrot_Set

[4] E. R. Miranda and A. Escalante, *Computer Sound Design: Synthesis Techniques and Programming*, 2nd ed. Oxford, UK: Newnes/Elsevier, 2001, chapter 4: Iterative algorithms, chaos, and fractals. Accessed: 2025-08-17.

[5] M. Burkey, "Structure in Chaos: An Exploration into the Mandelbrot Set," Whitman College, Walla Walla, WA, 2023, accessed: 2025-08-17. [Online]. Available: https://arminda.whitman.edu/_flysystem/fedora/2023-08/Structure_in_chaos_an_exploration_into_the_Mandelbrot_set.pdf

[6] R. L. Devaney, "The Complex Geometry of the Mandelbrot Set," Lecture notes, Prague, 2013, accessed: 2025-08-17. [Online]. Available: http://math.bu.edu/people/bob/papers/prague.pdf

[7] M. Susskind, "Mandelbrot-LogisticMap-EE (code repository)," GitHub, 2024–2025, accessed: 2025-08-17. [Online]. Available: https://github.com/matanou/Mandelbrot-LogisticMap-EE

[8] L. Keen and J. Kotus, "Dynamics of the family $\lambda \tan z$," *Conformal Geometry and Dynamics of the American Mathematical Society*, vol. 1, pp. 28–57, 1997.

[9] F. Monard, "Math 207 – spring '17 – lecture 20: Introduction to complex dynamics – mandelbrot and friends," Lecture notes, 2017.

[10] J. Milnor, "Hyperbolic components," Institute for Mathematical Sciences, Stony Brook University, Tech. Rep. IMS12-02, 2012, accessed: 19 Aug. 2025. [Online]. Available: https://www.math.stonybrook.edu/preprints/ims12-02.pdf

[11] C. Heiland-Allen, "Patterns in Embedded Julia Sets," mathr.co.uk (blog), 2017, accessed: 2025-08-17. [Online]. Available: https://mathr.co.uk/blog/2017-11-06_patterns_in_embedded_julia_sets.html

[12] A. Chéritat, "Computer-generated Math Pictures and Animation — Galerie I: Fractals," Personal website, Université de Toulouse, 2016, accessed: 2025-08-17. [Online]. Available: https://www.math.univ-toulouse.fr/~cheritat/wiki-draw/index.php/Mandelbrot_set

[13] E. Dummit, "Dynamics, Chaos, and Fractals (Part 5): Introduction to Complex Dynamics," Course notes, Math 3543, Northeastern University, 2023, accessed: 2025-08-17. [Online]. Available: https://dummit.cos.northeastern.edu/teaching_su23_3543/dynamics_5_introduction_to_complex_dynamics_v2.00.pdf

[14] E. W. Weisstein, "Logistic map," From MathWorld–A Wolfram Web Resource, 2024, accessed: 2025-08-14. [Online]. Available: https://mathworld.wolfram.com/LogisticMap.html

[15] G. Strang and E. Herman, "8.4: The logistic equation," Mathematics LibreTexts, 2024, accessed: 2025-08-14. [Online]. Available: https://math.libretexts.org/Bookshelves/Calculus/Calculus_(OpenStax)/08%3A_Introduction_to_Differential_Equations/8.04%3A_The_Logistic_Equation

[16] P. F. Verhulst, "Notice sur la loi que la population suit dans son accroissement," *Correspondance Mathématique et Physique*, vol. 10, pp. 113–121, 1838.

[17] G. Boeing, "Chaos Theory and the Logistic Map," Geoff Boeing Blog, 2015, accessed: 2025-08-17. [Online]. Available: https://geoffboeing.com/2015/03/chaos-theory-logistic-map/

[18] S. Lee, "Logistic Map Dynamics Explained," Number Analytics Blog, 2025, accessed: 2025-08-17. [Online]. Available: https://www.numberanalytics.com/blog/ultimate-guide-logistic-map-dynamical-systems

[19] R. M. May, "Simple mathematical models with very complicated dynamics," *Nature*, vol. 261, no. 5560, pp. 459–467, 1976.

[20] Nathaniel, "The Logistic Map," nathaniel.ai, n.d., accessed: 2025-08-17. [Online]. Available: https://www.nathaniel.ai/logistic-map/

[21] J. R. Chasnov, "8.1: Fixed points and stability," https://math.libretexts.org/Bookshelves/Differential_Equations/Differential_Equations_%28Chasnov%29/08%3A_Nonlinear_Differential_Equations/8.01%3A_Fixed_Points_and_Stability, Nov. 2021, accessed: 2025-08-16.

[22] F. Franco-Medrano, "Stability and chaos in real polynomial maps," *ResearchGate*, Jun. 2013, accessed: 2025-08-16. [Online]. Available: https://www.researchgate.net/publication/266026010_Stability_and_chaos_in_real_polynomial_maps

[23] A. Menasri, "Generalized logistic map and its applications," *AIP Advances*, vol. 15, no. 3, Mar. 2025, accessed: 2025-05-01. [Online]. Available: https://doi.org/10.1063/5.0263704

[24] A. Quillen, "PHY256 Lecture Notes on Bifurcations and Maps," https://astro.pas.rochester.edu/~aquillen/phy256/lectures/bif_maps.pdf, 2021, accessed: 2025-05-01.

[25] S. Bullett, "The Logistic Map, Period-doubling and Universal Constants," Lecture notes, Queen Mary University of London, accessed: 2025-08-17. [Online]. Available: https://webspace.maths.qmul.ac.uk/s.r.bullett/cf_chapter3.pdf

[26] Fiveable, "3.3 types of attractors – chaos theory," https://library.fiveable.me/chaos-theory/unit-3/types-attractors/study-guide/THSUlEJENrwcpgvX, 2024, accessed: 2025-08-16.

[27] J. Guo, "Analysis of chaotic systems," Oct. 2014, university of Chicago, Accessed: 2025-08-16.

[28] D. Kartofelev, "Lecture Notes 11 – Nonlinear Dynamics and Feigenbaum Constants," Tallinn University of Technology (YFX1560 course), 2013, accessed: 2025-08-17. [Online]. Available: https://www.tud.ttu.ee/web/dmitri.kartofelev/YFX1560/LectureNotes_11.pdf

[29] B. Luque, L. Lacasa, F. Ballesteros, and A. Robledo, "Analytical properties of horizontal visibility graphs in the feigenbaum scenario," *Chaos: An Interdisciplinary Journal of Nonlinear Science*, vol. 22, no. 1, p. 013109, Jan. 2012, accessed: 2025-08-17. [Online]. Available: https://arxiv.org/abs/1201.2514

[30] D. Tong, "2 discrete time," https://www.damtp.cam.ac.uk/user/tong/mathbio/mathbio2.pdf, accessed: 2025-08-16.

[31] A. G. Doz, "Theoretical-heuristic derivation sommerfeld's fine structure constant by feigenbaum's constant (delta): Periodic logistic maps of double bifurcation," https://vixra.org/pdf/1705.0355v2.pdf, Jun. 2017, accessed: 2025-08-16.

[32] R. O'Farrell, "Renormalization and universality in dynamics," https://math.uchicago.edu/~may/REU2024/REUPapers/O'Farrell.pdf, 2024, unpublished REU report; accessed: 2025-08-16.

[33] Wikipedia Contributors, "Logistic map," Wikipedia, Wikimedia Foundation, 2019, accessed: 2025-08-17. [Online]. Available: https://en.wikipedia.org/wiki/Logistic_map

[34] Y. Vorobets, "Math 614 dynamical systems and chaos," 2016, texas A&M University, Lecture notes.

[35] G. Rukavina, "Quadratic recurrence equations - exact explicit solution of period four fixed points functions in bifurcation diagram," arXiv:0802.2565 [math.DS], 2008, accessed: 2025-08-17. [Online]. Available: https://arxiv.org/abs/0802.2565

[36] P. Cvitanović, R. Artuso, R. Mainieri, G. Tanner, and G. Vattay, *Chaos: Classical and Quantum*, version 17 ed. Niels Bohr Institute, Copenhagen, 2017, chapter 5: Cycle Stability, Example 5.1, pp. 103–114. [Online]. Available: https://chaosbook.org/version17/chapters/invariants-2p.pdf

[37] University of Southampton, "Lecture 7 – logistic map and period doubling," 2012, lecture notes.

[38] R. Ghaziani, "Bifurcations of maps: Numerical algorithms and applications," Ph.D. dissertation, Ghent University, Ghent, Belgium, 2010.

[39] J. Sanders *et al.*, "Numerical bifurcation analysis of differential equations," 1985, accessed: 2025-08-17. [Online]. Available: https://webspace.science.uu.nl/~kouzn101/NBA/nba.pdf

[40] J. K. Hunter, "Index of /~hunter/intro_analysis_pdf," https://www.math.ucdavis.edu/~hunter/intro_analysis_pdf/ch1.pdf, 2015, accessed: 19 Aug. 2025.

[41] J. Marklof and C. Ulcigrai, "Dynamical systems and ergodic theory," https://people.maths.bris.ac.uk/~ip13935/dyn/CorinnaII.pdf, 2015, accessed: 19 Aug. 2025.

[42] A. Avila, M. Lyubich, and W. de Melo, "Regular or stochastic dynamics in real analytic families of unimodal maps," *Inventiones Mathematicae*, vol. 154, no. 3, pp. 451–550, 2003, accessed: 19 Apr. 2024. [Online]. Available: https://www.math.stonybrook.edu/preprints/ims01-15.pdf

[43] C. Ulcigrai, *Dynamical Systems and Ergodic Theory Part I: Examples of Dynamical Systems*. University of Zurich, Department of Mathematics, 2018, accessed: 19 Aug. 2025.

[44] A. Levy, "An algebraic proof of thurston's rigidity for maps with a superattracting cycle," 2014, accessed: 19 Aug. 2025. [Online]. Available: https://people.kth.se/~alonlevy/rigidity4.pdf

[45] L. Rempe, "Holomorphic dynamics, lecture iv," January 2008, accessed: 19 Aug. 2025. [Online]. Available: https://pcwww.liv.ac.uk/~lrempe/workshops/liv_jan_08/liverpool

[46] A. Cunningham, "Displaying the internal structure of the mandelbrot set," State University of New York at Buffalo, Tech. Rep., 2013, numerical Analysis MTH 537. [Online]. Available: https://www.acsu.buffalo.edu/~adamcunn/downloads/MandelbrotSet.pdf

[47] A. Douady and J. H. Hubbard, "On the dynamics of polynomial-like mappings," *Annales Scientifiques de l'École Normale Supérieure*, vol. 18, no. 2, pp. 287–343, 1985. [Online]. Available: http://www.numdam.org/item/ASENS_1985_4_18_2_287_0

[48] M. Lyubich, "On the dynamics of quadratic polynomials: Hyperbolicity and holomorphic motions," https://arxiv.org/abs/math/9201282, 1992, arXiv, Cornell University Library. Accessed 17 Aug. 2025.

[49] R. L. Devaney. (2022, May) 6.2: Misiurewicz points and the m-set self-similarity. Accessed: 2025-08-20. [Online]. Available: https://math.libretexts.org/Bookshelves/Scientific_Computing_Simulations_and_Modeling/The_Mandelbrot_and_Julia_sets_Anatomy_(Demidov)/6%3A_Periodic_and_preperiodic_points/6.2%3A_Misiurewicz_points_and_the_M-set_self-similarity

Appendices

Appendix A: Code Repository

The full source code for the logistic map and Mandelbrot visualisation tools developed for this essay is available on GitHub:

`https://github.com/matanou/Mandelbrot-LogisticMap-EE`

Instructions for running the programs are included in the repository's `README.md` file.

Appendix B: Logistic Map Explorer Interface

(i) Bifurcation Diagram Explorer

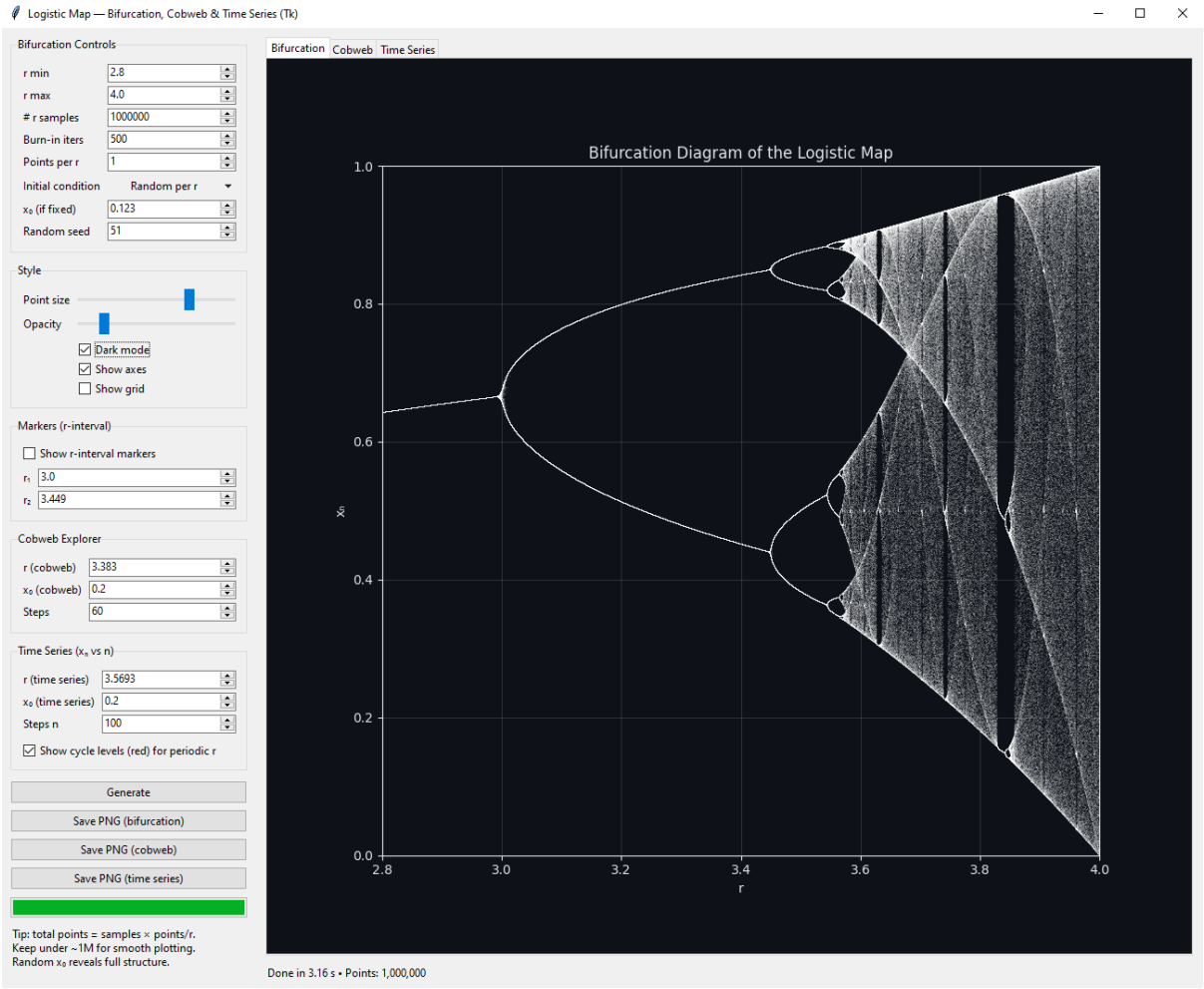

Figure 10: Screenshot of the logistic map explorer GUI, showing bifurcation diagram and parameter controls.

(ii) Time Series Explorer

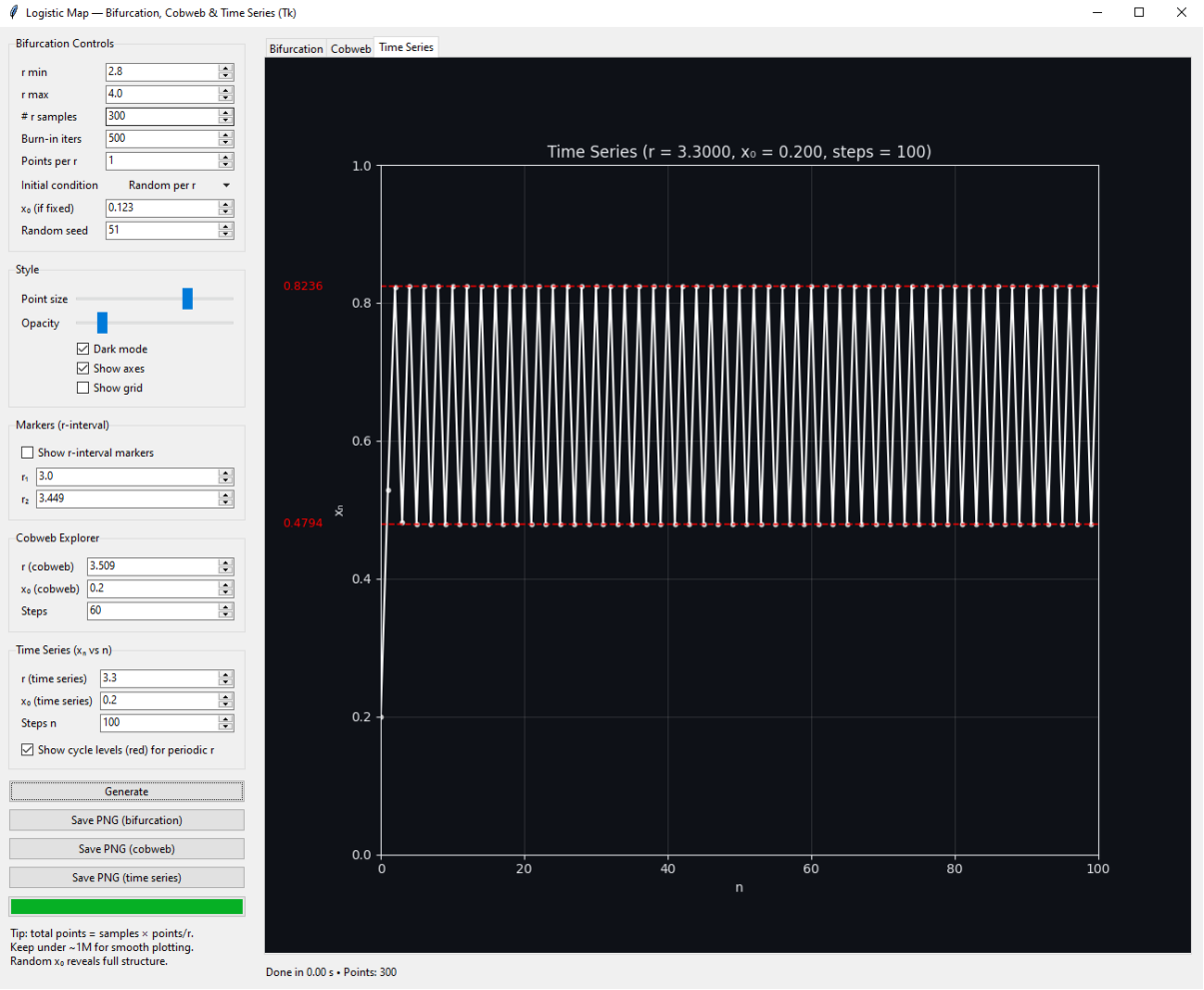

Figure 11: Screenshot of the logistic map explorer GUI, showing the evolution of the population x_n against time as steps n and parameter controls.

(iii) Cobweb Diagram Explorer

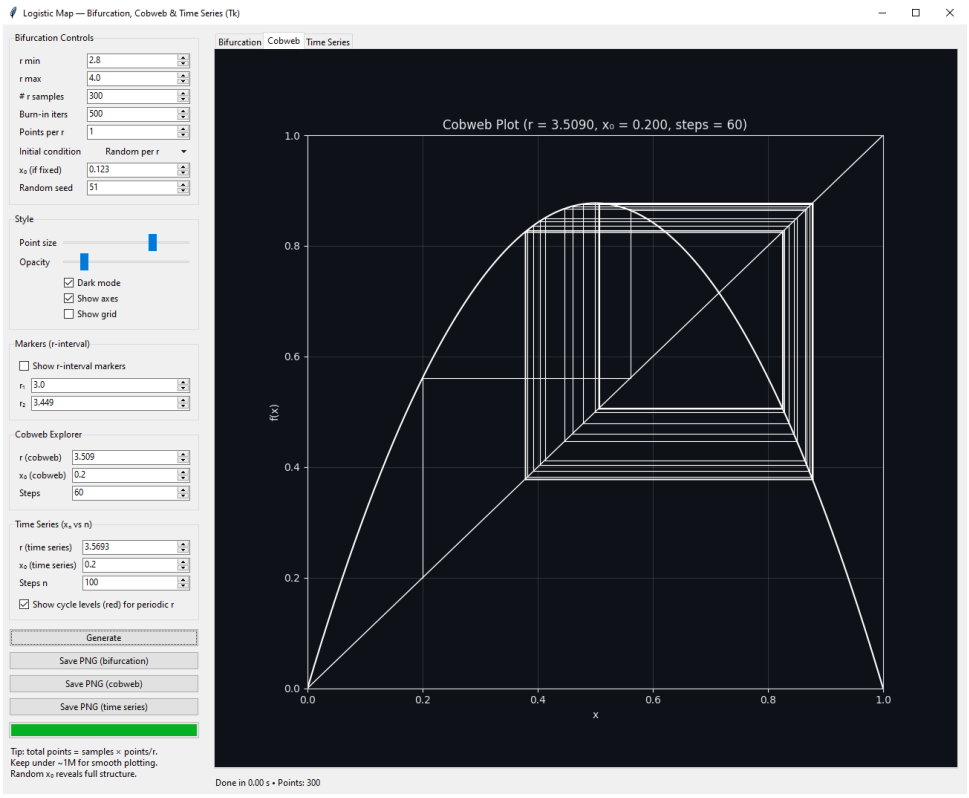

Figure 12: Screenshot of the logistic map explorer GUI, showing cobweb diagram and parameter controls.

Appendix C: Mandelbrot Explorer Interface

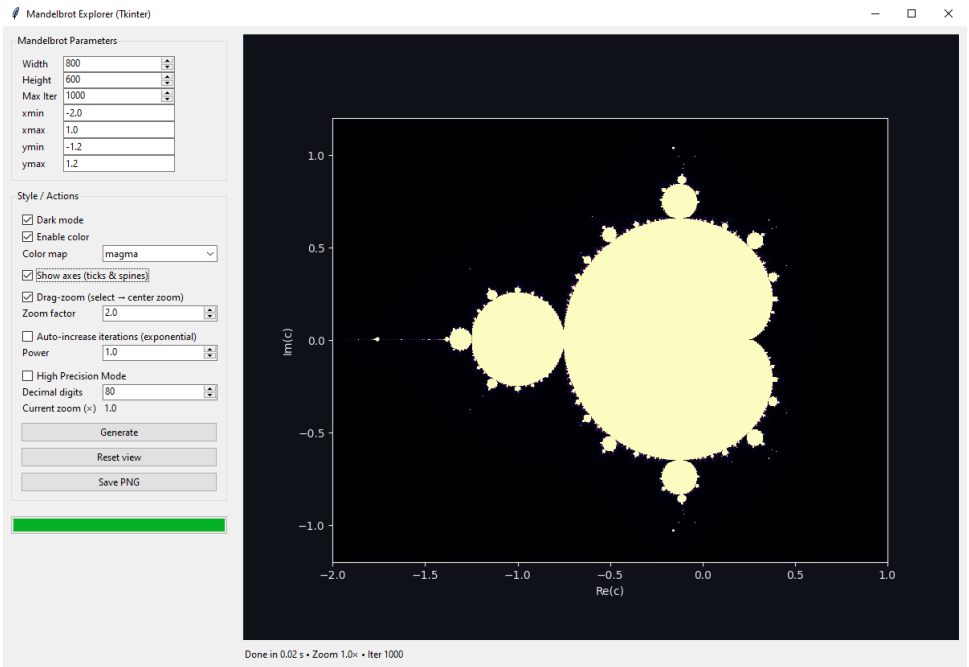

Figure 13: Screenshot of the Mandelbrot explorer GUI, showing parameter controls.

(i) Visualisation with colors

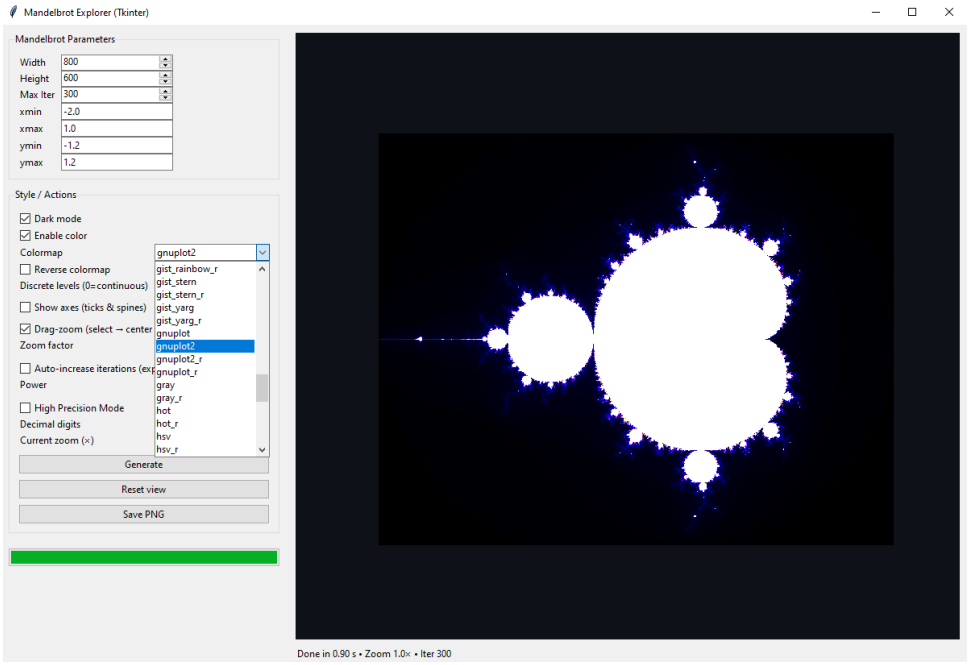

Figure 14: Screenshot of the Mandelbrot explorer GUI, showing colour controls (over 190 colour maps available).

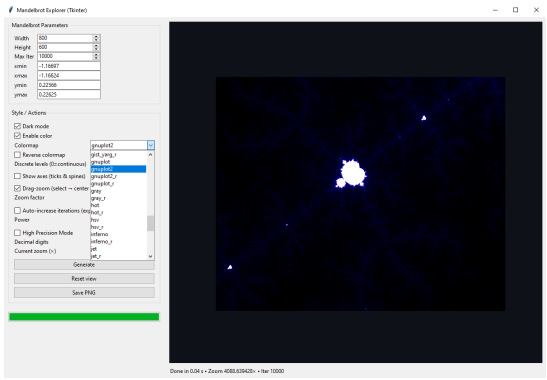

(a) Colour map 1.

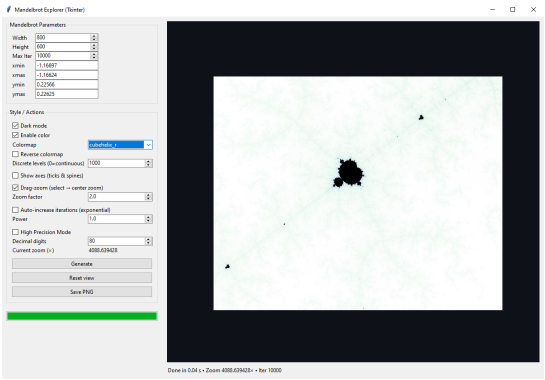

(b) Colour map 2.

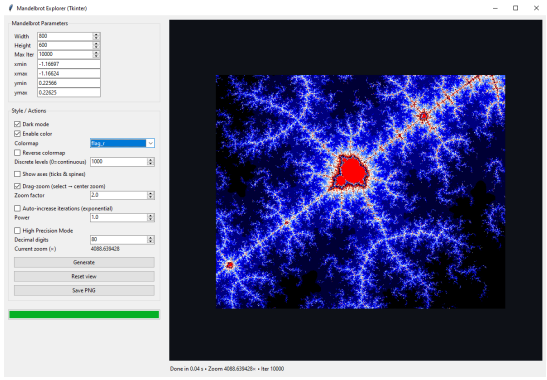

(c) Colour map 3.

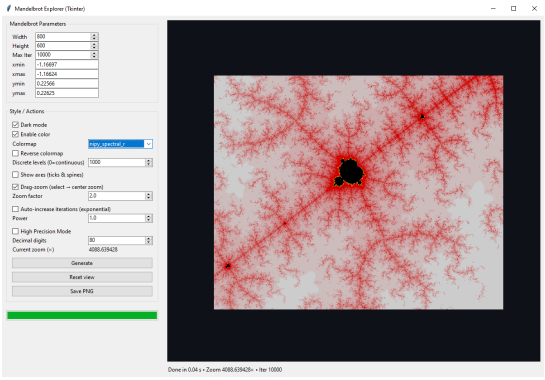

(d) Colour map 4.

Figure 15: Screenshots of the Mandelbrot explorer GUI, showing a zoomed-in section of the set rendered under different colour maps.

(ii) Zoom system

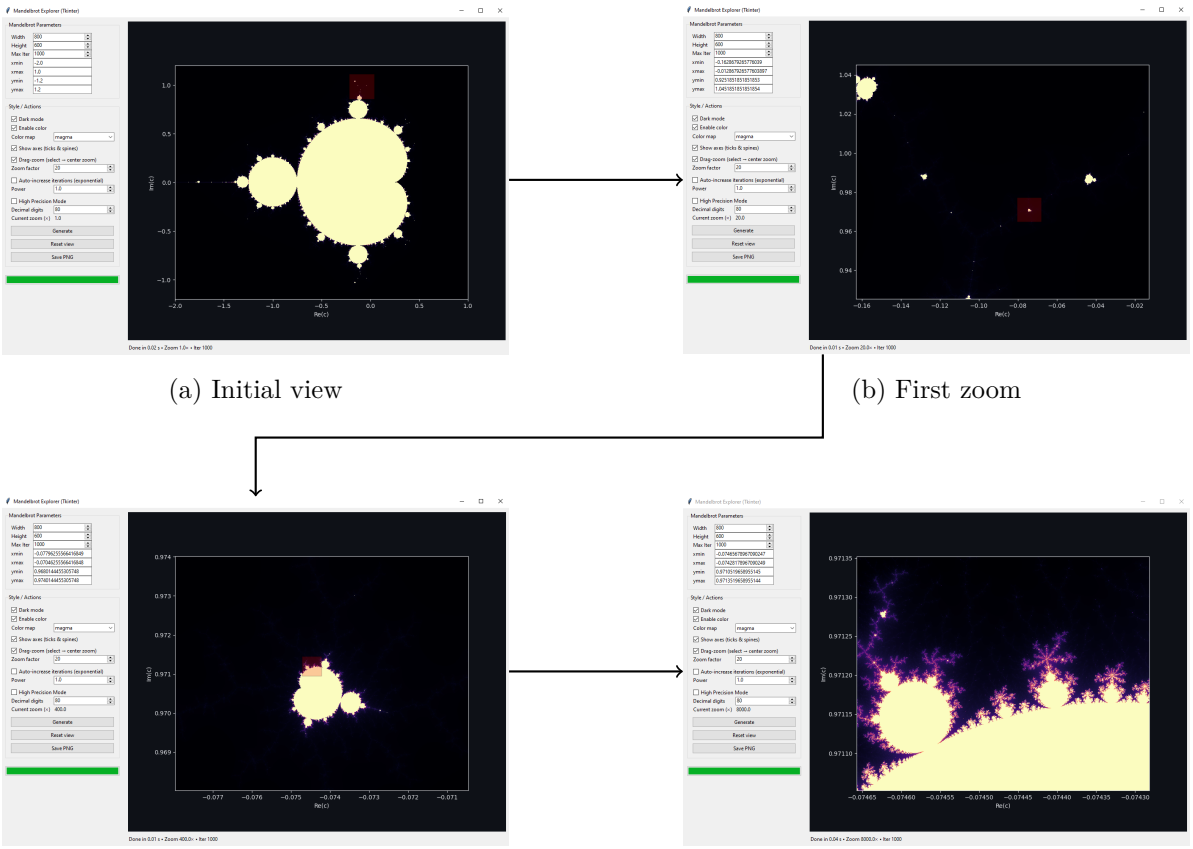

(a) Initial view

(b) First zoom

(c) Deeper zoom

(d) Deepest zoom

Figure 16: Screenshots of the Mandelbrot explorer GUI at successive zoom levels. Arrows indicate the order of magnification from (a) to (d).

Appendix D: Example Code Snippets

The following excerpts illustrate how the code generates trajectories for the logistic map and implements high-precision Mandelbrot calculations.

Logistic map iteration (Python).

```
def logistic_iter(x, r):
    return r * x * (1.0 - x)
```

Mandelbrot high-precision kernel (Python).

```
def mandelbrot_highprec(xmin, xmax, ymin, ymax, width, height, max_iter, dps):
    mp.dps = int(dps)
    image = np.zeros((height, width), dtype=np.uint16)
    ...
    return image
```